Zootaxa 4638 (2): 237–254
https://www.mapress.com/j/zt/

Article

ISSN 1175-5326 (print edition)
ZOOTAXA
ISSN 1175-5334 (online edition)

https://doi.org/10.11646/zootaxa.4638.2.4
http://zoobank.org/urn:lsid:zoobank.org:pub:2C04EF4A-B548-4338-9B8B-13D49A1F06BF

Description of *Eniacomorpha hermetiae* Delvare sp. n. (Hymenoptera, Chalcidoidea, Chalcididae) a pupal parasitoid of *Hermetia illucens* (L.) (Diptera, Stratiomyidae), and a potential threat to mass production of the fly as a feed supplement for domestic animals

GÉRARD DELVARE[1], ROBERT S. COPELAND[2,3] & CHRYSANTUS M. TANGA[2,4]
[1]*Centre de Coopération Internationale en Recherche Agronomique pour le Développement (CIRAD), Montpellier SupAgro, INRA, IRD, Univ. Montpellier, Montpellier, France*
[2]*International Centre of Insect Physiology and Ecology (ICIPE), P.O. Box 30772 - 00100, Nairobi, Kenya*
[3]*Department of Entomology, U. S. National Museum of Natural History, Smithsonian Institution, Washington DC, USA*
[4]*Corresponding author. E-mail:ctanga@icipe.org; Tel.: +254-20-8632000*

Abstract

Eniacomorpha hermetiae Delvare **sp. n**. (Hymenoptera, Chalcididae, Dirhininae), reared from pupae of black soldier fly (BSF), *Hermetia illucens* (Linnaeus, 1758) (Diptera, Stratiomyidae), is described and illustrated from Africa and compared with other similar species newly considered as forming the *ehrhorni* species-group within *Eniacomorpha* Girault, 1915. The newly described parasitic wasp may have a negative impact on efforts to mass produce BSF in Africa as a feed supplement for domestic animals. *Eniacomorpha* is removed from synonymy under *Dirhinus* Dalman, 1818, **revised status**, for the Afrotropical species of Dirhininae previously placed in *Dirhinus* subgenus *Pareniaca* Crawford, 1913. A checklist of the 10 recognized species of Afrotropical *Eniacomorpha* is given, of which 9 are new generic combinations.

Key words: Morphology, new parasitoid, Dirhininae, synonym, hosts, threat, feed supplement, black soldier fly, Kenya, Ghana

Introduction

There has been substantial interest in the use of black soldier fly (BSF) *Hermetia illucens* (Linnaeus) (Diptera, Stratiomyidae) in organic waste management and as a feed supplement for domestic animals. Adult flies are not pests, consume nothing but water or plant nectar, do not approach humans, do not bite or sting, and do not vector or disseminate any specific diseases (Čičková *et al*. 2015; Sheppard *et al*. 2002). Several studies have demonstrated that the voracious larvae of black soldier fly (BSFL) are capable of breaking down a wide variety of organic material such as manure (Sheppard 1983; Yu *et al*. 2009), rice straw (Zheng *et al*. 2012), food waste (Green & Popa 2012), distillers' grains (Webster *et al*. 2016), fecal sludge (Lalander *et al*. 2013; Banks *et al*. 2014), animal offal, kitchen waste and many more (Nguyen *et al*. 2015). According to Kim *et al*. (2011), the diversity of substrates that black soldier fly can process and the efficiency with which they do so may be the highest among the Diptera. The ability of BSF to convert low-value organic waste (municipal and household waste, agro-industrial waste, market waste and animal manures) into high-quality nutrient-rich animal-feed ingredients has recently gained momentum worldwide. This has rapidly generated innovative prospects for municipal solid waste management and the larvae of BSF are being promoted as an appropriate alternative to the expensive fishmeal or soybean meal in poultry, pig and fish feeds. Furthermore, the nitrogen-rich frass, resulting from the bioconversion process, is a valuable by-product when used as an organic fertilizer (Choi *et al*. 2009; Green & Popa, 2012), improving soil health and crop yield. Thus, BSF farming systems could benefit communities by providing opportunities for income generation, food and feed security, and sanitation. Despite the economic importance of BSF, several constraints hinder the sector from realizing its full potential. One of the impediments to sustainable and successful mass production systems is the

Accepted by G. Gibson: 10 Jun. 2019; published: 16 Jul. 2019

existence of parasitoids that attack BSF, and which may present a significant threat to BSF farming systems in the countries where they occur. However, the effects of parasitic wasps on BSF broodstock husbandry are not yet fully understood. Recently, Devic & Maquart (2015) reported that, in Ghana, *Dirhinus giffardii* Silvestri (Hymenoptera, Chalcididae), a well-known polyphagous parasitoid attacking Dipteran families including Tephritidae and Muscidae) (Wang & Messing 2004; Chiel & Kuslitzky 2015), also attacked BSF, and was thought to be the primary cause of the adult population decline they observed. Apart from this, the only other published report of parasitized BSF was that of Bradley *et al*. (1984) who reared species of *Trichopria* Ashmead (Hymenoptera, Diapriidae) from fly puparia in the southern United States). The present study reports the discovery of an undescribed species of chalcidid wasp parasitizing BSF in sub-Saharan Africa. This Afrotropical species, described below, is of considerable interest, especially as it was associated with a decline in the adult population in breeding cages of BSF.

Material and methods

Sampling. The occurrence of the parasitic wasp was first noticed in outdoor, adult rearing cages of BSF at the International Centre of Insect Physiology and Ecology, Nairobi, Kenya (Fig. 1). The cages contained fully-formed BSF pupae that were being kept for emergence. Adult wasps were collected from resting sites inside the cages. Immediately thereafter, several randomly selected 14 day-old BSF pupae were collected from the adult emergence cage and held individually in covered, 12-well flat bottom plates. Emerged parasitoids were removed daily from the wells and killed in 95% EtOH. Voucher specimens were placed in the collection of the Biosystematics Unit at ICIPE.

In addition, examination of Dirhininae individuals collected during an ongoing insect biodiversity study conducted by RSC revealed a single specimen of the new species that had been captured in a Malaise trap in Gede Forest (Fig. 2). Gede is one of a number of mostly small forests at the Kenya Coast, and part of the Coastal Forests of Eastern Africa biodiversity hotspot (https://www.cepf.net/our-work/biodiversity-hotspots/coastal-forests-eastern-africa).

Terms for morphology follow Bouček & Narendran (1981) and Delvare & Copeland (2018).

Imaging. All specimens were photographed using a digital microscope, Keyence VHX-5000 Photographs were digitally optimized (artifacts removal, background standardization) using the Photoshop® V program. The photos made with the aforementioned equipment were used for the measurements of the types (holotypes and some paratypes). Measurements were generally made in dorsal view but the antennal segments, the height of the head, the length and height of the eye, and the length of the malar space were measured in lateral view. Measurements were used to compute the ratios reported in the description. The acronyms designating some distances, namely OOD, POD are defined in Table 1 and Figs 4–6.

TABLE 1. Measurements of *Eniacomorpha hermetiae* Delvare **sp. n.**, paratype ♀ GDEL00463-0102 and paratype ♂ GDEL00463-0104 and *E. galesusaeformis* (Risbec) from CIRAD collection.

Measured parts \ Species	*Eniacomorpha hermetiae* ♀ (µm)	*Eniacomorpha hermetiae* ♂ (µm)	*Eniacomorpha galaesusaeformis* ♀ (µm)
width of head	1124	1114	1185
length of head (lateral view)	645	633	685
height of head = distance between apex of inner horn to lateral edge of oral fossa	1204	1393	1331
width of frontovertex	540	455	598
length of horn	224	238	293
depth of frontal depression	398	299	435
length of temple	273	258	348
distance between lateral ocelli (= POD)	123	86	158
distance between lateral ocellus to inner margin of eye (= OOD)	131	94	130
length of eye dorsal view	262	320	522
length of eye lateral view	515	492	511

.....continued on the next page

TABLE 1. (Continued)

Measured parts \ Species	*Eniacomorpha hermetiae* ♀ (µm)	*Eniacomorpha hermetiae* ♂ (µm)	*Eniacomorpha galaesusaeformis* ♀ (µm)
height of eye	434	410	413
distance from lower margin of eye to lateral edge of oral fossa	527	582	462
distance between apex of horn to dorsal margin of eye	239	393	293
length of mandible	268	348	380
combined length of pedicel + flagellum	1272	1291	1325
length of scape	783	791	813
width of scape	111	115	118
length of pedicel	179	152	183
width of pedicel	91	90	93
length of 1st flagellomere (= anellus)	91	54	119
width of of 1st flagellomere (= anellus)	88	90	91
length of 2nd flagellomere (= funicular 1)	166	185	195
width of 2nd flagellomere	104	106	111
length of 8th flagellomere (= funicular 7)	104	109	89
width of 8th flagellomere	143	136	147
clava length	215	223	213
clava width	140	136	153
length of mesosoma	2065	1957	2201
width of mesosoma	1228	1136	1261
length of pronotal collar	293	272	391
width of pronotal collar	1005	913	989
length of mesoscutum	543	500	511
length of mesoscutellum	652	630	679
width of mesoscutellum	707	592	707
propodeum submedian length	543	516	582
anteromedian areola of propodeum length	217	217	255
anteromedian areola of propodeum width	212	201	217
distance between hind corner of propodeum	511	462	554
length of fore wing	2696	2833	2910
width of fore wing	960	992	951
length of costal cell	1000	958	1000
length of marginal vein	744	800	811
length of hind wing	2158	2150	
length of hind wing	527	533	
length of metacoxa	773	474	
width of metacoxa	443	226	
length of metafemur	1135	674	
width of metafemur	724	442	
length pf petiole	184	254	179
width of petiole	426	459	522
length of gaster	1653	1443	1614
width of gaster	863	865	978
median length of first gastral tergite	1174	1004	1141
length of strigose area of first gastral tergite	479	422	495
width of strigose area of first gastral tergite	495	373	386

FIGURES 1, 2. Collecting sites. **1,** Outdoor rearing cages of *Hermetia illucens* on ICIPE campus, Nairobi, Kenya. **2**, Malaise trap at the Gede site, Kenya.

Measurements (Figs 4–6). The 'length of the head' is measured in lateral view. The 'height of the head' is the distance from the apex of the horn to the lateral corner of the oral fossa, the 'length of the malar space' is the distance from the lower eye margin to the lateral corner of the oral fossa. The submedian length of the propodeum is the distance between the apex of the mesoscutellum, which overhangs the postscutellum, and an imaginary line joining its hind corners on each side of the petiolar foramen. These structures provide easily viewable landmarks.

Collection acronyms used are: BMNH, Natural History Museum, London, UK; CIRAD, CIRAD collection in Centre de Biologie pour la Gestion des Populations (CBGP), Montferrier-sur-Lez, France; ICIPE, International Centre of Insect Physiology and Ecology, Biosystematics Unit, Nairobi, Kenya; MCSN, Museo Civico di Storia Naturale, Genova, Italia; MNB, Museum für Naturkunde, Berlin, Germany; MNHN, Muséum National d'Histoire Naturelle, Paris, France; MRAC, Musée Royal d'Afrique Centrale, Tervuren, Belgium; NMK, National Museums of Kenya, Nairobi, Kenya.

FIGURE 3. *Eniacomorpha hermetiae* Delvare **sp. n.**, paratype ♀.

Results

Taxonomy. Branstetter *et al*. (2017) recently resolved phylogenetic relationships among aculeate wasps and bees using a novel target capture approach. This strategy involved the sequencing and analyses of over one thousand Ultra Conserved Elements (UCE). Such a method provides massive molecular data using UCE as primers. It is now applied, by some colleagues of the CBGP, to the family Chalcididae. The results show that both the genus *Dirhinus* Dalman and the subgenus *Pareniaca* Crawford are polyphyletic (Cruaud *et al*. 2019; Delvare *et al*. 2019). In these analyses the Neotropical species of *Pareniaca* were retrieved as sister group of

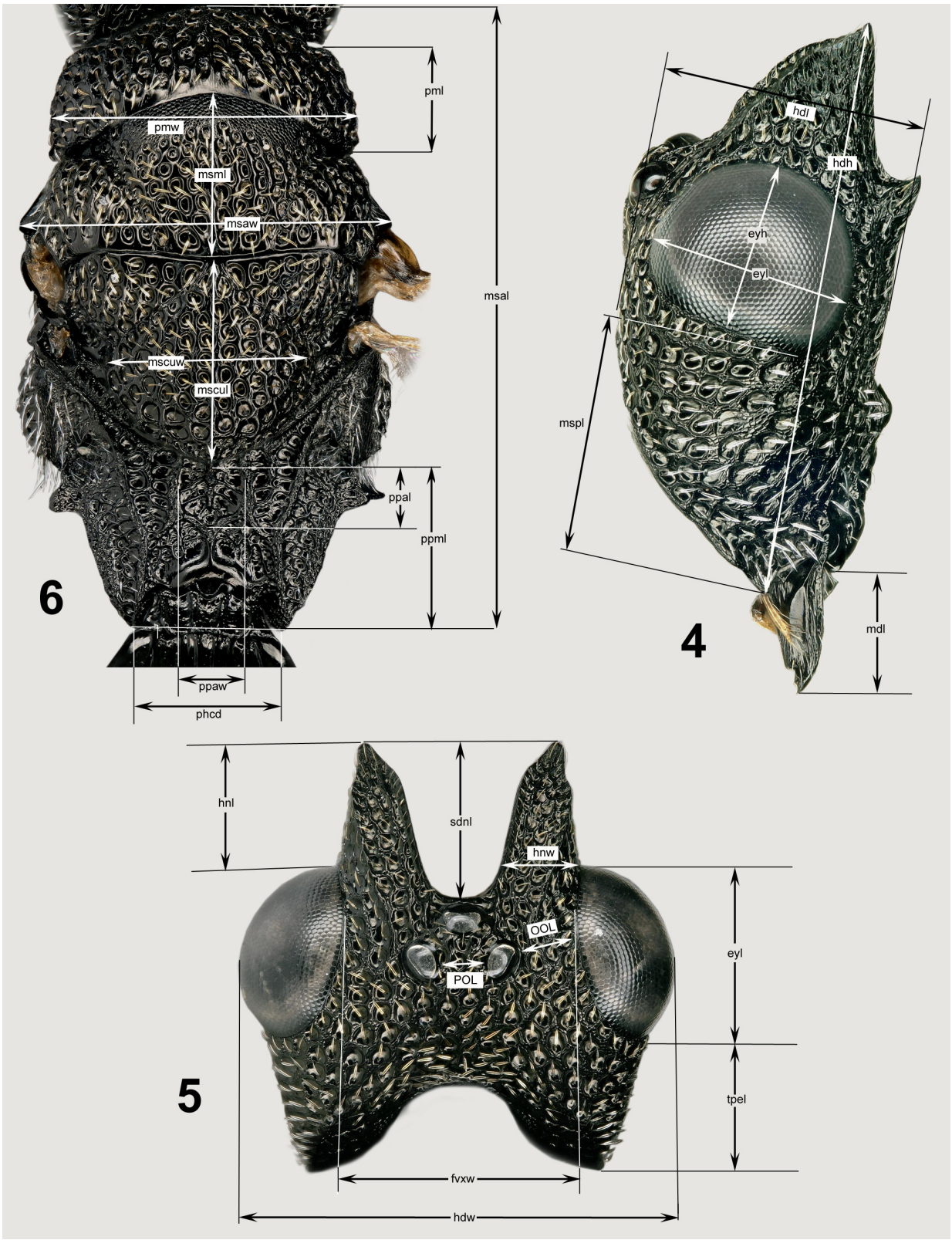

FIGURES 4–6. *E. hermetiae* ♀. Morphological terminology and measurements. **4**, head in lateral view. **5**, same in dorsal view. **6**, mesosoma in dorsal view. **Abbreviations**. **eyh**, eye height; **eyl**, eye length; **fvxw**, frontovertex width; **hdh**, head height; **hdl**, head length; **hdw**, head width; **hnl**, horn length; **hnw**, horn width; **mdl**, mandible length; **msal**, mesosoma length; **msaw**, mesosoma width; **msml**, mesoscutum length; **mscul**, mesoscutellum length; **mscuw**, mesoscutellum width; **mspl**, malar space length; **OOL**, ocellar-ocular length; **POL**, postocellar length; **phcd**, distance between adpetiolar projections of propodeum; **pml**, pronotum length; **pmw**, pronotum width; **ppal**, length of anteromedian areola of propodeum; **ppaw**, width of anteromedian areola of propodeum; **ppml**, median length of propodeum; **sdnl**, length of scrobal depression; **tpel**, temple length.

Hontalia Cameron, presently considered a subgenus of *Dirhinus* (Bouček 1992), while the single Afrotropical species sequenced—the present *E. hermetiae* described below—appears as the sister of a species possibly belonging to the genus *Aplorhinus* Masi. As *Pareniaca schwarzi* Crawford, the type species of *Pareniaca*, was described from the New World (Crawford), the Afrotropical species are necessarily excluded from it. *Eniacomorpha* Girault, described from Australia (Girault) and synonymized with *Dirhinus* by Bouček & Narendran (1981) is a possible replacement name. *Eniacomorpha vultur* Girault, its type species, was described from Australia and may fit the Afrotropical species that would be presently classified in *Dirhinus* subgenus *Pareniaca*.

Eniacomorpha Girault stat. rev.

Eniacomorpha Girault, 1915: 354. Original description. Type species *Eniacomorpha vultur* Girault, 1915 by original designation.

Diagnosis. Similar to *Pareniaca* in that the scrobal depression exhibits a secondary tooth; horn narrow and mostly sharp at apex in contrast to the wide scrobal depression; mandibles not elongate, clypeus bare or with short setae on either side, epicnemium distinctly elevated mesally with a narrow mesodiscrimenal groove that does not cross the ventral section of the epicnemial carina (Delvare & Copeland 2018: fig. 70), and hypopygium without long and paired apical setae. The anteromedian areola of the propodeum is at most somewhat longer than wide and the strigose area on the first gastral tergite is well expanded in the two dimensions, reaching at least one third of the dorsal surface of the tergite and occupying most of its width. These two characters distinguish *Eniacomorpha* from *Pareniaca*.

Eniacomorpha vultur Girault, 1915
(Figs 7, 8)

Eniacomorpha vultur Girault, 1915: 354. Original description ♂. Australia: Queensland, Gordonvale (Cairns).

Material examined. A female from Western Australia, identified as such by Z. Bouček, who examined the type series.

Diagnosis. Characters similar to those quoted by Delvare & Copeland (2018) for the *inflexus* group of *Pareniaca*, defined as including small species, with narrow and sharp horns regularly tapering from base to apex (Delvare & Copeland 2018: fig. 36); otherwise propodeum with anteromedian areola longer than wide and with parallel edges, and fore wing hyaline but bearing dark setae.

Checklist of *Afrotropical Eniacomorpha*

Eniacomorpha acuta (Schmitz, 1946) comb. n.

Pareniaca acutus Schmitz, 1946: 178–179. Original description ♂. Democratic Republic of Congo: Kivu, Rutshuru. Type material quoted: 2 ♂ including holotype ♂ n° 431 from Rutshuru, Kivu, 1285 m.

Type material. Holotype ♂ (MRAC) [examined].

Other material. **TOGO**: Massif du Kloto, 18.x.1998 (G. Delvare) (1 ♀ 1 ♂, in CIRAD).

Eniacomorpha antonii (Schmitz, 1946) comb. n.

Dirhinus antonii Schmitz, 1946: 171–173. Original description ♂. Democratic Republic of Congo: Rutshuru, Kivu rivière Kanzarue. Type material quoted: Holotype ♂ n° 1405 from Rutshuru, Kivu, 1285 m.

Type material. Holotype ♂ (MRAC) [examined].

Other material. **KENYA**: Western Province, Kakamega Forest near Rondo Guest House, 1630 m, 0.22767°N

34.88533°E, Malaise trap set across small permanent stream, 13-27.viii.2006 (Copeland R.) (1 ♀, in ICIPE); same data but 31.xii.2006-13.i.2007 (1 ♂, in ICIPE).

***Eniacomorpha ehrhorni* (Silvestri, 1913) comb. n.**

Dirhinus ehrhorni Silvestri, 1913: 132–133. Original description ♀. Nigeria: Olokomeji. Host: *Ceratitis giffardi* Bezzi. Holotype (by monotypy) quoted: 1 ♀.

Type material. Holotype ♀ (by monotypy) [not examined]

***Eniacomorpha galesusaeformis* (Risbec, 1957) comb. n.**
(Figs 9, 10, 15, 20, 21)

Paraniaca galaesusaeformis Risbec, 1957: 363. Original description ♂. Reunion Island. Holotype (by monotypy) quoted: 1 ♂ 'Forêt du Brulé de Mare-Longue, 30-I/3-II-1955.

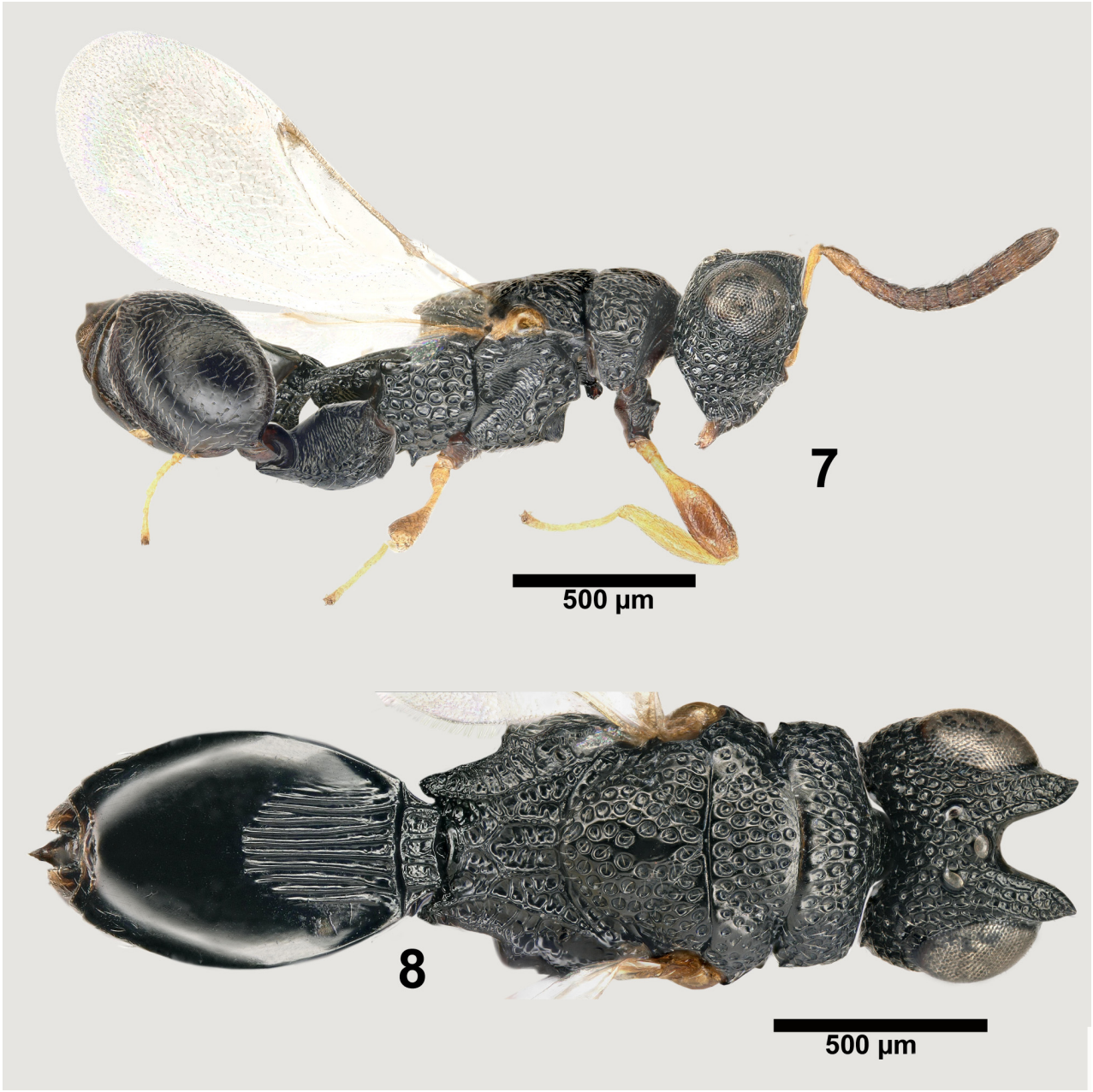

FIGURES 7, 8. *Eniacomorpha vultur* Girault ♀ from BMNH collection. **7**, lateral view. **8**, same in dorsal view.

Type material. Holotype ♂, extracted from slide ORSTOM 4.88 labelled in Risbec's handwriting 'Pareniaca galesusaeformis Risbec / La Reunion / Mare Longue / R. P.' [HT in red] and remounted on a card [examined].

Other material. **REUNION Island**: Bassin-Plat, ex Dacini, 22.iii.1997 (J.-F. Vayssières) (1 ♀, Ref. 14347, in CIRAD); same locality and collector, flying above laboratory culture of Dacini, 15.v.1997 (2 ♀, Ref. 14732(2), in CIRAD).

***Eniacomorpha inflexa (*Waterston, 1917) comb. n.**

Dirhinus inflexus Waterston, 1917: 178. Original description. Ghana. Host: *Glossina morsitans submorsitans* (Glossinidae).

Type material. Holotype ♀ (in BMNH Hym type 5-312) [examined].

Comment. The allotype ♂ (in MRAC) designated by Schmitz belongs to a close but different species.

***Eniacomorpha kivuensis* (Schmitz, 1946) comb. n.**

Pareniaca kivuensis Schmitz, 1946: 180. Original description ♀. Democratic Republic of Congo: Kivu, Rutshuru, rivière Kanzarue. Type quoted: Holotype ♀ n° 1649 from Rutshuru, (rivière Kanzarue), Kivu, 1200 m.

Type material. Holotype ♀ (in MRAC) [examined].

***Eniacomorpha madagascariensis* (Masi, 1947) comb. n.**

Pareniaca madagascariensis Masi, 1947: 71–74. Original description ♀. Madagascar.
Dirhinus madagascariensis (Masi): Bouček & Narendran, 1981: 232 (key, redescription, lectotype).

Type material. Lectotype ♀ designated by Bouček (1980) and validated here (in MNHN) [examined].

Other material. **MADAGASCAR**: **Majunga**, Ambovomany, Belambo, 20 km NW Port Berger, 33 m, 15°27.07"S 47°36.80"E, secondary growth on white sand, 7.i.2008, Irwin, Parker & Harin'hala (1 ♀ ref. MG-33-45 / CASLOT 036988, in CAS); same data but 27.i.2007, (2 ♀ 1 ♂ MG-33-04 / CASLOT 036971, in CAS); same data but 10.v.2007 (1 ♀ MG-33-20 / CASLOT 036976, in CAS); Namoroka village, Befatika, Andranovory, 7 km NW Vilandrano village, 122 m, 16°28.04'S 45°23.48'E, dense dry forest, 7.xii.2007, Irwin M. & Harin'hala leg. (2 ♀, MG-40B-11 / CASLOT 039533, one with ref. GDEL0337, in CIRAD);

***Eniacomorpha minima* (Schmitz, 1946) comb. n.**

Pareniaca minimus Schmitz, 1946: 180. Original description ♂. Democratic Republic of Congo: Kivu, Rutshuru. Type material quoted: Holotype ♂ n° 427 from Rutshuru, Kivu, 1285 m.

Type material. Holotype ♂ (in MRAC) [examined].

Other material. **TOGO**: Massif du Kloto, 18.x.1998 (G. Delvare) (1 ♂, in CIRAD).

***Eniacomorpha ugandensis* (Masi, 1947) comb. n.**

Pareniaca ugandensis Masi, 1947: 69–71. Original description ♂. Uganda: Bussu. Type material quoted: 1 ♂, Uganda: Bussu, 1909, E. Bayon leg.

Type material. Holotype ♂, by monotypy (in MCSN) [examined].

Other material. **BENIN**: Pobé, 17.xi.1993 (G. Delvare) (1 ♀, in CIRAD); **IVORY COAST**: Le Bolo near Guitry, 18.ix.1979 (J.-M. Maldès) (1 ♂, in CIRAD).

***Eniacomorpha hermetiae* Delvare sp. n.**
(Figs 3, 11–14, 16–19, 22–32)

Type material. **Holotype** ♀. **KENYA**: **Nairobi province**, ICIPE campus, R&D building, 1605 m, 1.22168°S

36.89624°E, ex outdoor colony of *Hermetia illucens*, xii.2015 (Tanga M. leg.) (in NMK). **Paratypes** (3 ♀ 3 ♂) with same data (♀ GDEL00463_0102-0101, in CIRAD); same data but specimens 'collected inside black soldier fly cage and reared from puparia'(9 ♀ 9 ♂, 5 ♀ 5 ♂ in NMK, 4 ♀ 4 ♂ in ICIPE); **Coast Province**, Gede Forest, indigenous forest, 3.30946°S 40.01941°E, Malaise trap in secondary forest, 17-31.x.2011 (R. Copeland) (1 ♀ in ICIPE).

Other material. **GHANA**: **Greater Accra Region**, Ashiama village, 298 m, 05°41'38.06" S 0°01'58.93" W, ex black soldier fly pupa, 2016 (Tanga M) (3 ♀ 3 ♂, in ICIPE).

Condition of holotype. Specimen complete, glued on rectangular card. Fore right leg [except coxa], left wings and hind leg glued separately.

Etymology. The name refers to the host, *Hermetia illucens*, from which the specimens were reared.

Description of female holotype (Fig. 3). Body length 4.7 mm. Body black including labrum, mandibles, all coxae and metafemur. Scape, pedicel, anellus and apex of clava, reddish; funiculars 1 and 2 brownish, remainder of funicle blackish. Trochantelli, femora and tibiae of fore and mid legs, brownish; tarsi pale yellow. Fore wing with brownish infuscation, the apical parts of basal and cubital folds and Rs fold entirely, darker; base of wing on costal cell, on a strip behind submarginal vein, on another one behind cubital fold, lighter; in contrast to infuscate membrane, median fold whitish; marginal cell and a spot beyond stigmal vein also somewhat lighter. Hind wing hyaline. Setae of fore wing and beyond venation on hind wing, dark. Lanceolate setae on vertex and pro- and mesonotum golden, silvery elsewhere; all hair-like setae silvery.

Head (Figs 11, 12, 16) 1.74× as wide as long, 0.93× as wide as high and 1.59× as high as long; eye 1.2× as long as high; temple as long as eye when latter is seen in dorsal view, with slightly convex lateral outline. Genal carina visible from above. Occiput, vertex and dorsal surface of horns densely punctured, the puncturation less coarse on horns. Setae on occiput and vertex lanceolate, adpressed and proclinate; setae on horns thin and about as long as diameter of punctures. Head with two horns mostly tapering near their narrowly rounded apex, their lateral margin being slightly sinuate there; lateral edge of horn separated from inner margin of eye by a row of punctures; width of horn at level of front margin of eye about two thirds the width of frontal depression. Dorsal margin of scrobal depression U-like with its end, in front of ocellar triangle, concave. Frontovertex 2.41× as wide as length of horn when the latter is measured from front margin of eye to apex of horn. Ocelli forming together an obtuse angle. Distance between lateral ocelli 0.94× as long as that of inter-ocellar distance. Posterior outline of head, between ocelli and upper end of genal carina, nearly straight. Anterior margin of horn with a moderately expanded tooth and forming an angle of about 60° with its dorsal margin. Inner margin of horn somewhat convex and visible from side. Sculpture and setation of gena, lateral surface of horn and adscrobal area identical to that of vertex and occiput. Inner margin of eye with a row of punctures. Outer margin of antennal scrobes straight except at level of tooth. Frontal depression reticulate on bottom, squamose reticulate on sides. Mandible with teeth broadly rounded at apex in front view but sharply so in side view. Labrum triangular, bearing a few setae on disc and with a short marginal fringe. Clypeus as a bulging surface somewhat wider than high and with 2 setae on either side. No malar groove or malar carina. Lateral outline of gena somewhat convex. Genal margin forming an acute and sharp angle with lateral edge of oral fossa.

Antenna (Fig. 17). Scape linear, progressively tapering from base to apex, about half as long as height of head as defined above. Combined length of pedicel plus flagellum as long as head width. Pedicel, anellus (first flagellomere) and first funicular respectively 1.96×, 1.02× and 1.59× as long as wide; followings funiculars progressively decreasing in length, with 8th flagellomere [= last funicular segment] 0.73× as long as wide and 1.38× as wide as 2nd flagellomere. Setation of flagellum short and adpressed, each segment with one row of multiporous plate sensilla (MPS), except F1 having a few MPS at base. Clava ovoid, 1.53× as long as wide, narrowly rounded at apex and bearing a small apical area of micropilosity.

Mesosoma (Figs 22–24) 1.68× as long as wide, dorsally flattened. Pro- and mesonotum densely punctured with smooth interspaces and bearing lanceolate and adpressed setae, except on posterior third of mesoscutellum where setae hair-like. Pronotal collar transverse, 3.43× as wide as long, progressively merging to collus, its sides convex; setae at least as long as diameter of punctures, reclinate on mesal surface, oriented inwards laterally. Lateral panel of pronotum flat, densely punctured. Mid lobe of mesoscutum with a densely reticulate front strip; the lanceolate setae oriented towards a median line. Notaulus a punctured groove. Lateral lobe only slightly less densely punctured than mid lobe but more coarsely so, bearing reclinate setae while they are proclinate on the axilla. Mesoscutellum 0.92× as long as wide, virtually flat, angulate anteriorly because axillar grooves almost join each other on transscutal line, and with a small mucro posteriorly, overhanging postscutellum. Propodeum with surface virtually horizontal, exhibiting dense secondary areolation but bottom of areolae smooth; walls separating areolae thick and micro-sculptured;

setation thin and suberect, absent on anteromedian and adpetiolar areolae; anteromedian areola cordiform, as long as wide, followed by a complete and regular median carina; sublateral areolae triangular, adpetiolar areolae broadly rounded anteriorly; spiracle situated within a setose fovea; spiracular tooth projecting, not sharp and somewhat raised upwards. Lateral panel of prepectus densely reticulate and dull; ventral belt with laterally compressed median tooth with convex edge in side view. Mesepisternum with mesodiscrimenal groove not interrupting epicnemial carina, widening above, quite narrow ventrally, situated on the top of a projecting elevation; adscrobal area, ventral shelf of mesepisternum and mesepimeron densely punctured, bearing adpressed, lanceolate setae; femoral scrobe with longitudinal carinulae alternating with coriaceous strips, entirely coriaceous on upper third. Metepimeron coarsely punctured and with adpressed, lanceolate setae same as mesepisternum and mesepimeron; subcoxal and precoxal teeth on posterior margin projecting and sharp. Metepisternum rugose-areolate in front of petiolar foramen, reticulate-strigose anteriorly, with vestigial posterior projection.

Legs (Figs 3, 29). Procoxa with anterobasal fovea accommodating temple, the fovea carinately margined on outer side. Profemur thickened. Mesofemur strongly inflated apically. Mesotibia compressed laterally. Mesotarsus 0.80× as long as tibia. Metacoxa 1.74× as long as wide, with broad apicodorsal flange having a regularly rounded edge; coxa densely strigose dorsally to apex, sparsely punctured ventrally and densely setose laterally. Metafemur quite broad, only 1.57× as long as wide and with strongly convex dorsal margin at base; short and wide basal tooth visible on ventral margin of metafemur before serrulation; small inner tooth present near base; disc of femur with moderately dense punctulation, the interspaces between points about twice as wide as their diameter; setae thin and adpressed, about twice as long as interspaces between points.

Wings (Figs 25, 26). Fore wing 2.81× as long as wide; marginal vein 0.74× as long as costal cell. Basal and cubital folds as well as basal cell bare; Rs fold with 2–3 rows of setae. Costal cell with a row of setae on underside, with a few additional setae near apex. Marginal cell with 12 irregularly distributed setae on upper side. Median fold and underside of wing membrane from level of base of marginal vein with microtrichiae on underside, the membrane with hair-like setae on upper side. Apex of submarginal vein with 3 sensilla placodea, stigmal vein with 4 aligned sensilla.

Metasoma (Figs 27, 28, 30). Petiole bare, with dorsal surface transverse, 2.3× as wide as long, with sublateral ridges converging backwards; foveae smooth; petiole with a sharp, hook-like basiventral tooth. Gaster 1.91× as long as wide, 1st gastral tergite large, 0.71× as long as gaster, longitudinally strigose on basal third, the strigose surface about as long as wide with slightly convex posterior limit, and including nine primary ridges (joining the basal transverse carina), lacking secondary crests; outer ridges straight, similar to the other ones; tergite punctulate and with short setae on sides near apex. Following tergites much shorter with progressively more concave posterior margins; each tergite bearing a row of setae and a transverse strip of punctulation. Hypopygium reaching apex of gaster, with 2 submedian rows of setae, the apical row hardly longer than the basal.

Male 4.2 mm. In most respect similar to the female but with horns and flagellum longer and pedicel shorter than in female; the proportions that differ from female are quoted below.

Head (Figs 13, 14, 18) exactly as wide as long and 0.60× as wide as high; frontovertex 1.91× as wide as length of horn; temple only 0.81× as long as eye in dorsal view.

Antenna (Fig. 19). Combined length of pedicel plus flagellum 1.56× as long as head width. Pedicel, anellus (first flagellomere) and first funicular respectively 1.70, 0.61 and 1.74× as long as wide; following funiculars progressively decreasing in length, with 8th flagellomere [= last funicular segment] 0.80× as long as wide and 1.28× as wide as 2nd flagellomere.

Mesosoma (Fig. 31) 1.72× as long as wide, with dorsum somewhat convex; mesoscutellum 0.92× as long as wide

Metasoma (Figs 31, 32). Petiole bare, with dorsal surface transverse, 1.8× as wide as long. Gaster 1.67× as long as wide, 1st gastral tergite longitudinally strigose on basal two fifths, the strigose surface 1.13× as long as wide.

Variation. The specimens from Ghana have the flagellum, fore and mid legs darker, clearly brown. No other variation was found.

Diagnosis. *Both sexes*. Head coarsely punctured on frons, vertex, occiput and gena (Figs 11, 12); horn narrow, tapering near apex where its inner edge is sinuous; apex of horn sharp; marginal carina of frontal depression U-like, concave in front of ocellar triangle; outer edge of horn separated from inner eye margin by a row of punctures; inner and outer edges of horn slightly convex when seen in lateral view; temple straight on side. Lanceolate setae golden on vertex, occiput, pronotum and most of mesoscutellum (Fig. 22). Anteromedian areola of propodeum about as

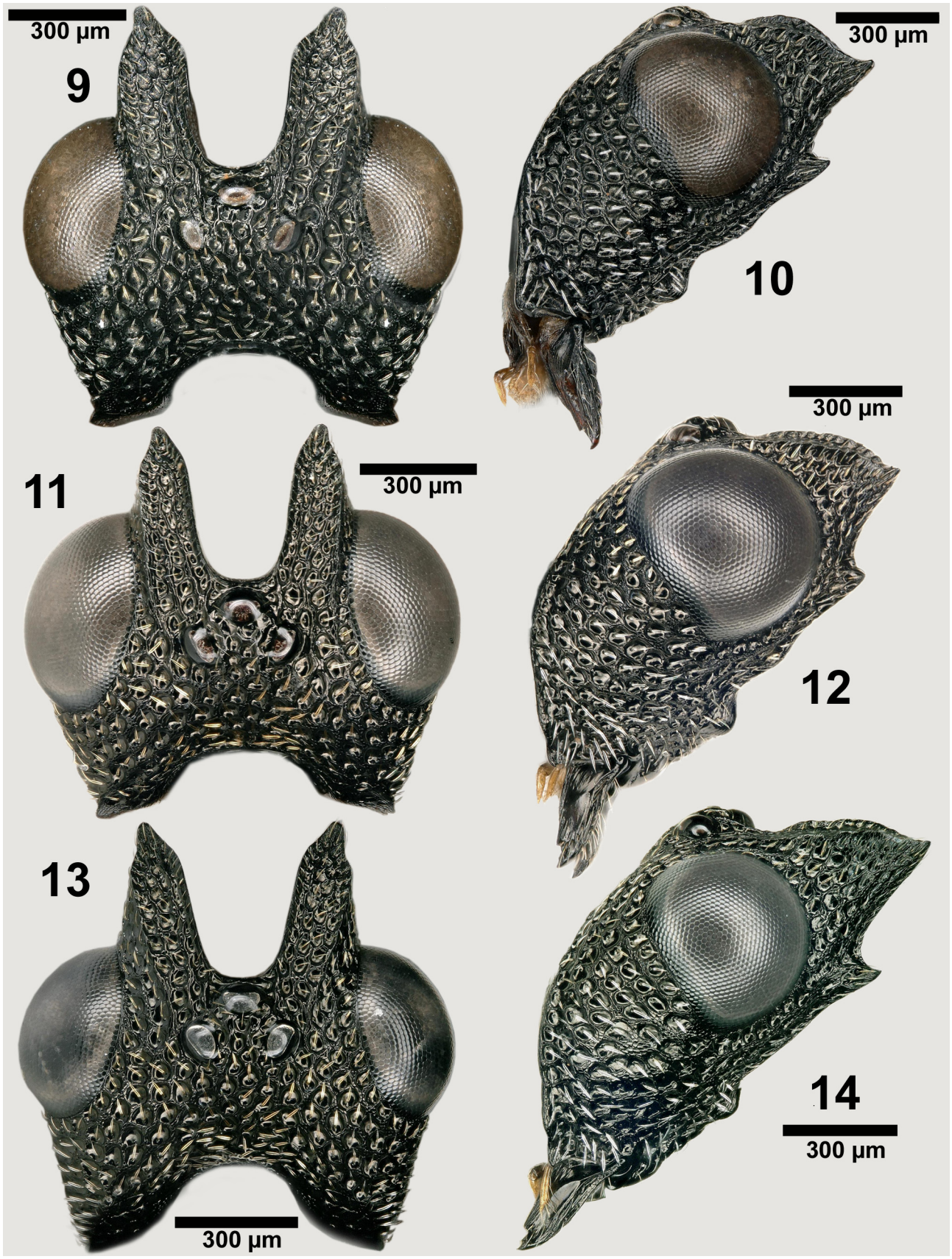

FIGURES 9–14. **9 and 10**. *Eniacomorpha galesusaeformis* (Risbec) ♀. **9**, head in dorsal view. **10**, same in lateral view. **11 and 12**. *E. hermetiae* ♀. **11**, head in dorsal view. **12**, same in lateral view. **13 and 14**. *E. hermetiae* ♂. **13**, head in dorsal view. **14**, same in lateral view.

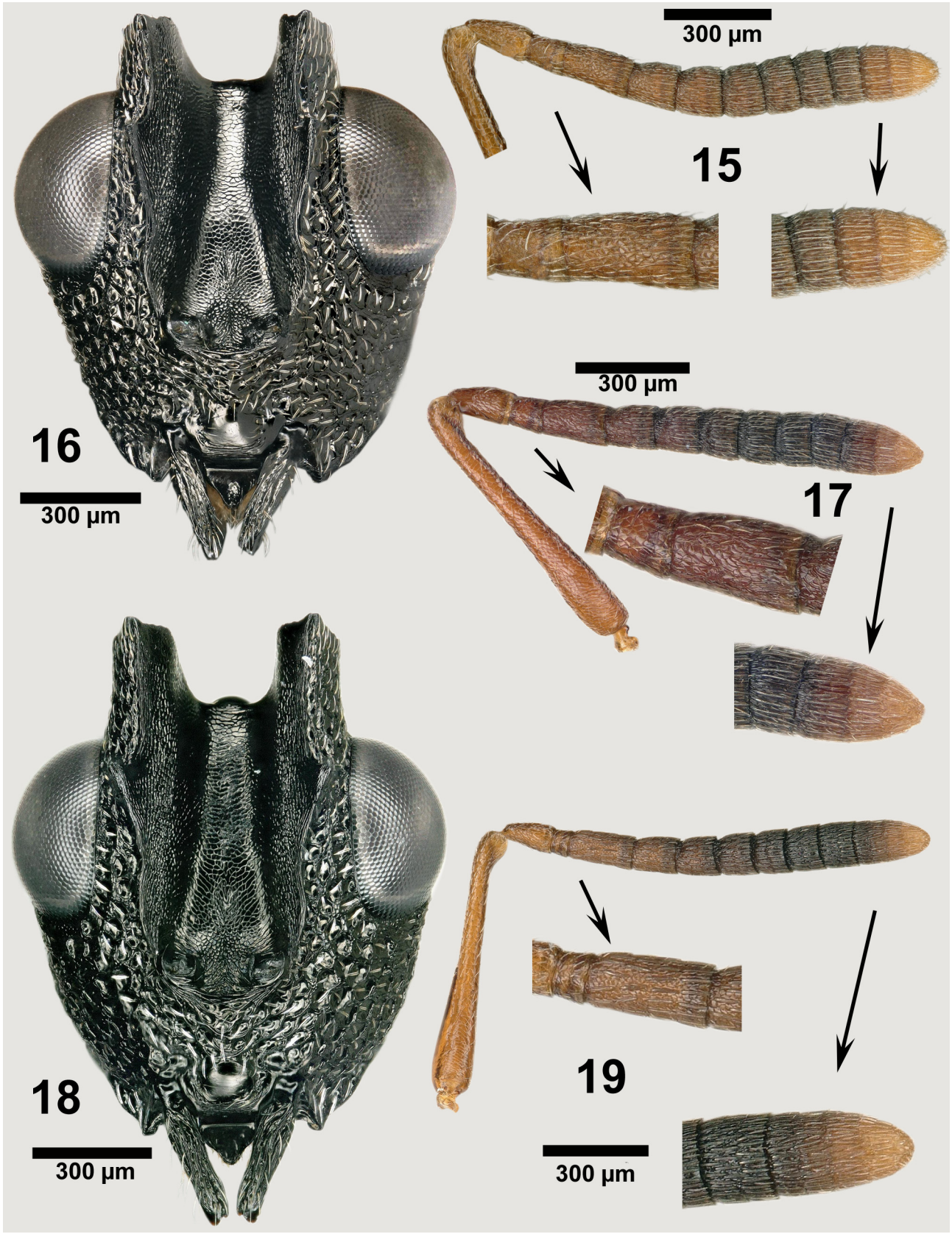

FIGURES 15–19. **15.** *E. galesusaeformis* ♀, antenna with base flagellum and clava enlarged. **16 and 17**. *E. hermetiae* ♀. **16**, head in frontal view. **17**, antenna with base flagellum and clava enlarged. **18 and 19**. *E. hermetiae* ♂. **18**, head in frontal view. **19**, antenna with base flagellum and clava enlarged.

FIGURES 20–28. **20 and 21**. *E. galesusaeformis* ♀. **20**, fore wing. **21**, same, wing glued on white card. **22–28**. *E. hermetiae* ♀. **22**, mesosoma in dorsal view. **23**, prepectus and mesepisternum. **24**, mesosoma in ventral view. **25**, fore wing. **26**, same, wing glued on white card. **27**, metasoma in lateral view. **28**, apex of metasoma in ventral view.

long as wide with convex lateral edges. Femoral depression of mesopleuron coarsely sculptured, strongly strigose at mid-height. Fore wing with membrane brownish except at base, on marginal cell and a spot on front margin of wing beyond venation; setae dark; Rs fold setose (Figs 25, 26). Petiole strongly transverse with basoventral tooth sharp, hook-like. Strigose surface of first gastral tergite not half of tergite length (Fig. 30). *Male* with flagellum filiform (Fig. 19).

Host. Reared from pupae of *Hermetia illucens* (L.) (Diptera, Stratiomyidae).

Distribution. Ghana and Kenya.

Recognition. *Comparison with other Afrotropical Eniacomorpha. Eniacomorpha ehrhorni*, *E. galesusaeformis* and *E. hermetiae* can be included in a separate group (= *ehrhorni* group) that can be distinguished from the other Afrotropical *Eniacomorpha* by the following characters:

- from *E. ugandensis* and *E. minimus* (and a few other undescribed species) by the partly infuscate fore wing in species of the *ehrhorni* group ***versus*** wing entirely hyaline;
- from *E. madagascariensis* (and a few other undescribed species) by the presence in the ehrhorni group of a row of punctures separating the outer margin of the horn from the inner eye margin ***versus*** outer margin of horn tangent to inner eye margin;
- from *E. kivuensis*, *E. inflexa* and *E. acuta* by the longer temple in species of the *ehrhorni* group, at least 0.60× as long as the eye [in dorsal view], with its side not or hardly convex ***versus*** temples shorter, at most 0.50× as long as the eye, with the side markedly convex;
- from two undescribed species by the margins of the horn converging toward each other [in dorsal view] in species of the *ehrhorni* group, the horn exhibiting an acute apex and, in addition, the secondary tooth often larger and sharper ***versus*** margins of horn parallel, not converging toward each other, the horn being narrowly rounded at apex and with a small secondary tooth;

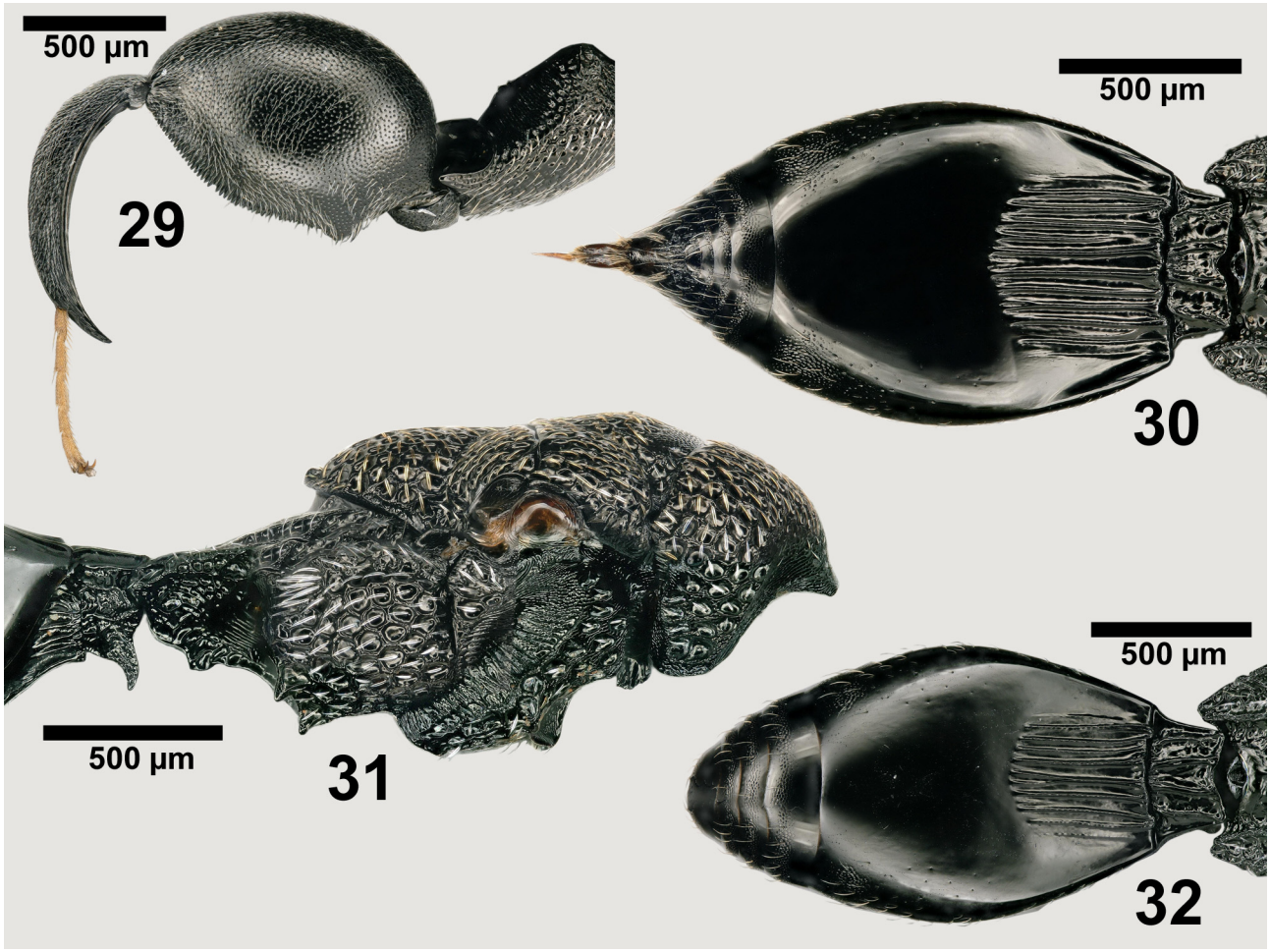

FIGURES 29–32. **29 and 30**. *E. hermetiae* ♀. **29**, hind leg. **30**, metasoma in dorsal view. **31 and 32**. *E. hermetiae* ♂. **31**, mesosoma and petiole in lateral view. **32**, metasoma in dorsal view.

- from *E. antonii* by the mesosoma being less elongate in the *ehrhorni* group species, with the anteromedian areola of the propodeum not or hardly longer than wide and having convex edges ***versus*** mesosoma and propodeum markedly elongate, the anteromedian areola being much longer than wide and having parallel edges;

Within the *ehrhorni* group, *E. galesusaeformis* and *E. hermetiae* have the secondary tooth along the scrobal depression larger and sharper than that of *E. ehrhorni*, the eye relatively smaller with its margin distant from both the hind and front margin of the head ***versus*** secondary tooth small, eye quite large, with its front margin very close to that of the frons in *E. ehrhorni*.

Detailed comparison with E. galesusaeformis to which *E. hermetiae* is very close (but see also the ratios given in Table 2).

E. hermetiae. Female. Head less high than in *E. galesusaeformis*, about 1.59× as high as long (Figs 12, 16). Ocelli larger with distance between median to lateral ocellus about 1/3× diameter of median ocellus (Fig. 11). Horn with both dorsal edges weakly convex when seen from lateral view. First funicular 1.6× as long as wide (Fig. 17). Combined length of pedicel plus flagellum as long as head width. Clava narrowly rounded at apex.

E. galesusaeformis. *Female*. Head higher than in *E. hermetiae*, 2.20× higher than long (Fig. 10). Ocelli smaller with distance between median to lateral ocellus ca. 3/5× the diameter of median ocellus (Fig. 9). Horn with both edges more convex when seen from lateral view. Funicular 1 (2nd flagellomere) 1.75× as long as wide (Fig. 15). Combined length of pedicel plus flagellum 1.12× as long as head width. Clava broadly rounded at apex.

TABLE 2. Ratios from measurements quoted in Table 1.

Ratios E. hermetiae F	*Eniacomorpha hermetiae* ♀	*Eniacomorpha hermetiae* ♂	*Eniacomorpha galesusaeformis* ♀
head width: head length	1.743	1.760	1.730
head height: head length	1.588	2.201	1.943
head width: head height	0.934	0.800	0.890
eye length: eye height (lateral view)	1.187	1.200	1.237
POD: OOD	0.938	0.913	1.208
temples length: eye length (dorsal view)	1.042	0.808	0.667
horn length: eye length (dorsal view)	0.854	0.744	0.563
frontovertex width: horn length	2.415	1.914	2.037
Combined length pedicel + flagellum: head width	1.023	1.559	1.119
scape length: head height	0.483	0.569	0.611
pedicel length: pedicel width	1.964	1.697	1.957
anellus length: anellus width	1.037	0.606	1.309
Fl2 length: Fl2 width	1.594	1.744	1.759
Fl8 length: Fl8 width	0.727	0.800	0.609
Fl8 width: Fl2 width	1.375	1.282	1.325
clava length: clava width	1.535	1.640	1.391
mesosoma length: mesosoma width	1.681	1.722	1.746
mesoscutum width: pronotum width	1.222	1.244	1.275
pronotal collar width: pronotal collar length	3.426	3.360	2.528
mesoscutum length: pronotal collar length	1.852	1.840	1.306
mesocutellum length: mesoscutellum width	0.923	1.064	0.962
gaster length: mesosoma length	0.800	0.737	0.733
metacoxa length: metacoxa width	1.744	2.093	
metafemur length: metafemur width	1.567	1.524	
fore wing length: fore wing width	2.808	2.857	3.060
marginal vein length: costal cell length	0.744	0.835	0.811
petiole length: petiole width	0.432	0.554	0.344
gaster length: gaster width	1.915	1.668	1.650
first gastral tergite length: gaster length	0.710	0.696	0.707
strigose surface of GT1 length: strigose surface of GT1 width	0.968	1.132	1.282

Acknowledgements

The authors express their appreciation to Natalie Dale-Skey (BMNH), Roberto Poggi and Maria Tavano (MCSN), Claire Villemant and Agnièle Touret-Alby (MNHN) and Eliane De Coninck (MRAC) for the loan of types and their kind and helpful welcome during the visits of GD. RSC thanks the director of ICIPE for her continuing support of our project on biodiversity of insects, and the director of the Kenya Forest Service for permission to sample in Gede Forest. This research was financially supported by the Netherlands Organization for Scientific Research, WOTRO Science for Global Development (NWO-WOTRO) (ILIPA–W 08.250.202), Federal Ministry for Economic Cooperation and Development (BMZ) (ENTONUTRI–81194993), The Rockefeller Foundation (SiPFeed—2018 FOD 009), the Canadian International Development Research Centre (IDRC) and the Australian Centre for International Agricultural Research (ACIAR) (INSFEED—Phase 2: Cultivate Grant No: 108866-001) through the International Centre of Insect Physiology and Ecology. We also gratefully acknowledge the ICIPE core funding provided by UK Aid from the Government of the United Kingdom; Swedish International Development Cooperation Agency (SIDA); the Swiss Agency for Development and Cooperation (SDC); Federal Ministry for Economic Cooperation and Development (BMZ), Germany, and the Kenyan Government. *The views expressed herein do not necessarily reflect the official opinion of the donors.*

References

Banks, I.J., Gibson, W.T. & Cameron, M.M. (2014) Growth rates of black soldier fly larvae fed on fresh human faeces and their implication for improving sanitation. *Tropical Medicine and International Health*, 19, 14–22. https://doi.org/10.1111/tmi.12228

Bouček, Z. (1992) The New World genera of Chalcididae. *In*: Delvare, G. & Bouček, Z. (Eds.), On the World Chalcididae (Hymenoptera). *Memoirs of the American Entomological Institute*, 53, pp. 49–117.

Bouček, Z. & Narendran, T.C. (1981) Indian chalcid wasps (Hymenoptera) of the genus *Dirhinus* parasitic on synanthropic and other Diptera. *Systematic Entomology*, 6, 229–251. https://doi.org/10.1111/j.1365-3113.1981.tb00438.x

Bradley, S.W., Booth, D.C. & Sheppard, D.C. (1984) Parasitism of the Black Soldier Fly by *Trichopria* sp. (Hymenoptera: Diapriidae) in poultry houses. *Environmental Entomology*, 13, 451–454. https://doi.org/10.1093/ee/13.2.451

Branstetter, M.G., Danforth, B., Pitts, J.P., Faircloth, B.C., Ward, P.S., Buffington, M.L., Gates, M.W., Kula, R.R. & Brady, S.G. (2017) Phylogenomic insights into the evolution of stinging wasps and the origins of ants and bees. *Current Biology*, 27, 1019–1025. https://doi.org/10.1016/j.cub.2017.03.027

Chiel, E. & Kuslitzky, W. (2015) Diversity and abundance of house fly pupal parasitoids in Israel, with first records of two *Spalangia* species. *Environmental Entomology*, 45 (2), 283–291. https://doi.org/10.1093/ee/nvv180

Choi, Y.C., Choi, J.Y., Kim, J.G., Kim, M.S., Kim, W.T., Park, K.H., Bae, S.W. & Jeong, G.S. (2009) Potential usage of food waste as a natural fertilizer after digestion by *Hermetia illucens* (Diptera: Stratiomyidae). *International Journal of Industrial E* https://doi.org/10.1093/ee/13.2.451*ntomology*, 19, 171–174.

Crawford, J.C. (1913) Descriptions of new Hymenoptera. No 7. *Proceedings of the United States National Museum*, 45, 309–317. https://doi.org/10.5479/si.00963801.45-1984.309

Cruaud A., Delvare, G., Nidelet, N., Sauné, L., Ratnasingham, S., Chartois, M., Blaimer, B., Gates, M., Brady, S., Faure, S., van Noort, S., Rossi, J.P. & Rasplus J.-Y. (2019) Resolving the tree of life of poorly known groups: Exploration of phylogenomic incongruence in chalcid wasps (Hymenoptera: Chalcidoidea: Chalcididae). *Systematic Biology*. [submitted]

Čičková, H., Newton, G.L., Lacy, R.C. & Kozánek, M. (2015) The use of fly larvae for organic waste treatment. *Waste Management*, 35, 68–80. https://doi.org/10.1016/j.wasman.2014.09.026

Delvare, G. & Copeland, R.S. (2018) Four-horned wasps, description of some remarkable *Dirhinus* Hymenoptera, Chalcididae) from Kenya, with a discussion of their taxonomic placement. *Zootaxa*, 4374 (3), 301–349. https://doi.org/10.11646/zootaxa.4374.3.1

Delvare, G., Cruaud, A., Nidelet, S., Sauné, L. & Rasplus, J.-Y. (2019) Ultra-Conserved Elements and morphology provide congruent evidence for a new generic classification of the Chalcididae (Hymenoptera, Chalcidoidea). *Systematic Entomology*. [in preparation]

Devic, E. & Maquart, P.-O. (2015) *Dirhinus giffardii* (Hymenoptera Chalcididae), parasitoid affecting Black Soldier Fly produc-

tion systems in West Africa. *Entomologia*, 3 (284), 25–27.
https://doi.org/10.4081/entomologia.2015.284
Girault, A.A. (1915) Australian Hymenoptera Chalcidoidea—XIV. The family Chalcididae with descriptions of new genera and species. *Memoirs of the Queensland Museum*, 4, 314–365.
Green, T.R. & Popa, R. (2012) Enhanced ammonia content in compost leachate processed by black soldier fly larvae. *Applied Biochemistry and Biotechnology*, 166, 1381–1387.
https://doi.org/10.1007/s12010-011-9530-6
Kim, W., Bae, S., Park, K., Lee, S., Choi, Y., Han, S. & Koh, Y. (2011) Biochemical characterization of digestive enzymes in the black soldier fly, *Hermetia illucens* (Diptera: Stratiomyidae). *Journal of Asia-Pacific Entomology*, 14, 11–14.
https://doi.org/10.1016/j.aspen.2010.11.003
Lalander, C., Diener, S., Magri, M.E., Zurbrugg, C., Lindstrom, A. & Vinneras, B. (2013) Faecal sludge management with the larvae of the black soldier fly (*Hermetia illucens*)—From a hygiene aspect. *Science of the Total Environment*, 458, 312–318.
https://doi.org/10.1016/j.scitotenv.2013.04.033
Masi, L. (1947) Nuovo contributo all conoscenza dei Dirhinini (Hymen. Chalc.). *Eos*, *Revista Española di Entomologia*, *Madrid*, 23, 39–78.
Nguyen, T.T.X., Tomberlin, J.K. & Vanlaerhoven, S. (2015) Ability of black soldier fly (Diptera: Stratiomyidae) larvae to recycle food waste. *Environmental Entomology*, 44, 406–410.
https://doi.org/10.1093/ee/nvv002
Risbec, J. (1957) Hyménoptères Proctotrupidae et Chalcidoidea. *Mémoires de l'Institut Scientifique de Madagascar*, Série E, 8, 321–366.
Schmitz, G. (1946) Chalcididae (Hymenoptera Chalcidoidea). *In*: *Exploration du Parc National Albert*, *Mission G. F. de Witte (1933-1935)*. *Fascicule 48*. Institut des Parcs Nationaux du Congo Belge, Bruxelles, pp. 1–191, 17 pls.
Sheppard, C. (1983) Housefly and lesser fly control utilizing the black soldier fly in manure management-systems for caged laying hens. *Environmental Entomology*, 12, 1439–1442.
https://doi.org/10.1093/ee/12.5.1439
Sheppard, D.C., Tomberlin, J.K., Joyce, J.A., Kiser, B.C. & Sumner, S.M. (2002) Rearing methods for the black soldier fly (Diptera: Stratiomyidae). *Journal of Medical Entomology*, 39, 695–698.
https://doi.org/10.1603/0022-2585-39.4.695
Silvestri, F. (1913) Viaggio in Africa per cercare parassiti di mosche dei frutti. *Bollettino del Laboratorio di Zoologia Generale e Agraria della R. Scuola Superiore d'Agricoltura, Portici*, 8, 1–164.
Wang, X.-G. & Messing, R.H. (2004) Potential interactions between and egg- or larval-pupal parasitoids of tephritid fruit flies. *Environmental Entomology*, 33 (5), 1313–1320.
https://doi.org/10.1603/0046-225X-33.5.1313
Waterston, J. (1917) Chalcidoidea bred from *Glossina* in the northern territories, Gold Coast. *Bulletin of Entomological Research*, 8, 178–179.
https://doi.org/10.1017/S0007485300037585
Webster, C.D., Rawles, S.D., Koch, J.F., Thompson, K.R., Kobayashi, Y., Gannam, A.L., Twibell, R.G. & Hyde, N.M. (2016) Bio-ag reutilization of distiller's dried grains with solubles (DDGS) as a substrate for black soldier fly larvae, *Hermetia illucens*, along with poultry by-product meal and soybean meal, as total replacement of fish meal in diets for nile tilapia, *Oreochromis niloticus*. *Aquaculture Nutrition*, 22, 976–988.
https://doi.org/10.1111/anu.12316
Yu, G.H., Chen, Y.H., Yu, Z.N. & Cheng, P. (2009) Research progress on the larvae and prepupae of black soldier fly *Hermetia illucens* used as animal feedstuff. *Chinese Bulletin of Entomology*, 46, 41–45.
Zheng, L.Y., Hou, Y.F., Li, W., Yang, S., Li, Q. & Yu, Z.N. (2012) Biodiesel production from rice straw and restaurant waste employing black soldier fly assisted by microbes. *Energy*, 47, 225–229.
https://doi.org/10.1016/j.energy.2012.09.006